Volume 4, Issue 2, December 2018 ISSN 2356-8569

ACADEMY Publishing Center

Journal of Renewable Energy and Sustainable Development

RESD

Academy Publishing Center
Journal of Renewable Energy and Sustainable Development (RESD)
First edition 2015

Permissions may be sought directly Academy Publishing Center,
Arab Academy for Science, Technology, and Maritime Transport,
Abu Kir Campus, Alexandria, EGYPT
P.O. Box: Miami 1029
Tel:(+203) 5622366/88 – EXT 1069 and (+203) 561 1818
Fax: (+203) 561 1818
Web Site: http://apc.aast.edu

Volume 4, Issue 2, December 2018

ISSN: 2356-8518 Print Version

ISSN: 2356-8569 Online Version

ACADEMY Publishing Center

Journal of Renewable Energy and Sustainable Development

RESD

Renewable Energy and Sustainable Development (RESD) is a biannual international peer-reviewed journal which presents a global forum for dissemination of research articles, case studies and reviews focusing on all aspects of renewable energy and its role in sustainable development. The topics of focal interest to RESD include, but are not limited to, all aspects of wind energy, wave/tidal energy, solar energy, as well as energy from biomass and biofuel. The integration of renewable energy technologies in electrical power networks and smart grids is another topic of interest to RESD. Experimental, computational and theoretical studies are all welcomed to RESD.

Sustainable development is a multidisciplinary advancing to the center of energy research with the declaration of UN millennium development goals for the first time in 2000, and continued to constitute a challenge in energy technologies in the past decade. RESD is mainly interested in case studies of sustainable development and its relation to transition economies in the Middle East, Africa, Asia and Oceania.

RESD has an outstanding editorial board of eminent scientists, researchers and engineers who contribute and enrich the journal with their vast experience in different fields of interest to the journal. The journal is open-access with a liberal Creative Commons Attribution-Non Commercial-4.0 International License. Which preserves the copyrights of published materials to the authors and protects it from unauthorized commercial use or derivation. The journal is financially supported by Arab Academy for Science, Technology and Maritime Transporting in order to maintain quality open-access source of research papers on renewable energy and sustainable development.

Editorial Committee

Peer Review Process

Peer review is an objective process at the heart of good scholarly publishing and is carried out on all reputable scientific journals. Our referees therefore play a vital role in maintaining the high standards of Renewable Energy and Sustainable Development (RESD) and all manuscripts are peer reviewed following the procedure outlined below.

Overall process for publishing a paper will be taken approximately 4 months after initial submission. Reviewing process will take about 2 months, and then publishing process will not exceed 2 months.

1. Initial manuscript evaluation

The Editor first evaluates all manuscripts. It is rare, but it is entirely feasible for an exceptional manuscript to be accepted at this stage. Those rejected at this stage are insufficiently original, have serious scientific flaws, have poor grammar or English language, or are outside the aims and scope of the journal. Those that meet the minimum criteria are passed on to at least 2 experts for review.

Authors of manuscripts rejected at this stage will normally be informed within 2 to 3 weeks of receipt.

2. Type of Peer Review

This journal employs single blind reviewing, the author identity is disclosed to the referee, while the referee remains anonymous throughout the process.

3. How the referee is selected

Referees are matched to the paper according to their expertise. Our database is constantly being updated. RESD has a policy of using single blind refereeing (as detailed in the previous section), with neither referee from the country of the submitting author. We welcome suggestions for referees from the author though these recommendations may or may not be used.

4. Referee reports

Referees are asked to evaluate whether the manuscript support followings key points related to scientific content, quality and presentation:

4.1. Technical

Scientific merit: notably scientific rigour, accuracy and correctness.

Clarity of expression; communication of ideas; readability and discussion of concepts.

Sufficient discussion of the context of the work, and suitable referencing.

4.2. Quality

Originality: Is the work relevant and novel?

Motivation: Does the problem considered have a sound motivation? All papers should clearly demonstrate the scientific interest of the results.

Repetition: Have significant parts of the manuscript already been published?

Length: Is the content of the work of sufficient scientific interest to justify its length?

4.3. Presentation

Title: Is it adequate and appropriate for the content of the article?

Abstract: Does it contain the essential information of the article? Is it complete? Is it suitable for inclusion by itself in an abstracting service?

Diagrams, figures, tables and captions: Are they essential and clear?

Text and mathematics: Are they brief but still clear? If you recommend shortening, please suggest what should be omitted.

Conclusion: Does the paper contain a carefully written conclusion, summarizing what has been learned and why it is interesting and useful?

Referees are not expected to correct or copyedit manuscripts. Language correction is not part of the peer review process.

5. How long does the review process take?

Typically the manuscript will be reviewed within 3 months. Should the referees' reports contradict one another or a report is unnecessarily delayed a further expert opinion will be sought. All our referees sign a conflict of interest statement. Revised manuscripts are usually returned to the initial referees within 1 week. Referees may request more than one revision of a manuscript.

6. Editorial decisions

After peer review and referee recommendation, the editor-in-chief, with the assistance of the associate editor, will study the paper together with reviewer comments to make one of the following decisions.

Accept

Accept pending minor revision: no external review required

Reject/Resubmit: major revisions needed and a new peer-review required

Reject

Digital Object Identifier

The RESD is supported by Digital Object Identifier, DOI for each article from Cross Ref.

The Code of the DOI of each article consists of the following format:

10.21622/RESD.YYYY.VV.I.PPP

Where

10.21622	= Journal Identifier
RESD	= Journal name
YYYY	= Four digits for the year
VV	= Two digits for the Volume Number
I	= One digit for the Issue Number
PPP	= Three digits for the Number of the first page of the article

To look for the paper on line, search for this link
http://dx.doi.org/10.21622/RESD.YYYY.VV.I.PPP

Table of Contents

http://dx.doi.org/10.21622/RESD.2018.04.2.056

Sustainable Energy and Mobility as Drivers for the Economic Growth in the Mediterranean Islands

Professor Theocharis Tsoutsos
Director, Renewable and Sustainable Energy Lab
School of Environmental Engineering, Technical University of Crete
Polytecheneioupolis, GR 73100 Chania
Email: theocharis.tsoutsos@enveng.tuc.gr

The “greening” of the inhabitant Mediterranean islands is crucial in order to build a sustainable future. Furthermore, the islands consist a major global tourism destination, so the potential minimization of their carbon footprint is essential for the success of the Paris Agreement.
The islands have the potential to be frontrunners in the clean energy transition by adopting new technologies, implementing and demonstrating innovative solutions, also for transport.
However, there is a number of challenges for their smooth operation and sustainability, such as:

- Energy safety, space use, road safety, air quality and noise pollution are some transport related issues that islands have to cope with.
- Islands are attractive as touristic destinations, feature a high pressure to their fantastic nature and sensitive ecosystems, which need special care and protection
- The seasonal fluctuation in their operation impacts on the design of their necessary infrastructure (ports, roads, energy supply systems)
- Although they should comply with the most recent national and international commitments, they are missing capacity, resources and social preparation for these changes.

Fostering a Mediterranean insular sustainable energy and mobility approach will also support the development of innovative, quality tourism products and services to make destinations even more attractive, as well as to address the mobility needs of citizens and visitors.

The above approach was discussed during the Public Hearing organized by the Network of the Insular Chambers of Commerce and Industry of the European Union (INSULEUR) and the Renewable and Sustainable Energy Systems Lab of the Technical University of Crete (ReSEL-TUC) on Friday 8th of June 2018 at the premises of the European Economic and Social Committee (EESC), in Brussels. The event was organised in partnership with the EESC and was supported by the Conference of Peripheral Maritime Regions (CPMR) and the European Small Islands Federation (ESIN).

About Professor Theocharis Tsoutsos

Theocharis Tsoutsos is Professor, Head of Renewable and Sustainable Energy Lab (ReSEL) (2005- now), School of Environmental Engineering, Technical University of Crete; also the Director of Graduate Programme "Environmental Engineering" (2014-2018) and the Coordinator of the TUC-Energy Group (2013-2017) and the Head of Development Dept (Centre for Renewable Energy Sources & Energy Saving - CRES (1992- 2005). He is a Member of Management Council (RMEI -réseau méditerranéen des ecoles d'ingénieurs et de management, 2018-now). He has coordinated 40+ projects on RES and energy efficiency; participated in 100+ totally.
Professor Tsoutsos is the author of 300+ scientific publications in international journals, conference proceedings; He has 3,000+ citations h-factor:25 (Scopus); 29 (Google Scholar). He is also Editorial Board Member in the following peer-review international journals: Energies (2017-); AIMS Energy (2013-); Int. J. of Sust Built Environment (2015-now). He is a Project evaluator in European Research Council (ERC), REA (EC), Erasmus-Mundus (EC), GSRT (GR), State Scholarship Foundation (GR), Research Promotion Foundation (CY), Swiss National Science Foundation (SNSF); New Eurasia Foundation (RU); Netherlands Organization for Scientific Research (NL); Welsh Government (UK).

Journal of Renewable Energy and Sustainable Development (RESD) Volume 4, Issue 2, December 2018 - ISSN 2356-8569
http://dx.doi.org/10.21622/RESD.2018.04.2.057

Implementation of MPPT Algorithm for Single-Stage Grid-Connected Photovoltaic System Using Incremental Conductance Method

Mustafa Abu-Zaher[1], Yousry Atia[2], Farag K . Abo Elyousr[3], Emad H. El-Zohri[1]
[1] Electrical Dept, Faculty of Industrial Education, Sohag University, Egypt.
[2] Electronics Research Institute, Giza, Egypt.
[3] Electrical Engineering Dept, Faculty of Engineering, Assiut University, Egypt.
mostafa.abuzaher@yahoo.com

***Abstract* -** This paper presents simulation and implementation of maximum power point tracking algortim for single stage three-phase grid-connected PV system by using incremental conductance method.The maximum efficiency is realized when PV works at its maximum power point, which is contingent on irradiation and temperature. Since the irradiation and temperature always change with time, a PV system which is able to track the maximum power point needs to be established to produce more energy. The INC method shows a superior performance, lower oscillation and it took three seconds to match MPP best time to give stability to the system. The control strategy is supported out using MATLAB/Simulink and experimentally validated with a dSPACE MicroLabBox controller.

***Keywords* -** Photovoltaic, Maximum power point tracking, Single-stage, Grid-connected,Incremental conductance.

I. INTRODUCTION

In the present development, rapid innovation with advance technology has enlarged the demand for modern resourses of electric power [1]. Installation of additional power sources pose challenges due to the exhaustion of conventional fossil fuels in addition to environmental pollution and global roasting. This necessitated the exploitation of renewable sources of energy, such as identical solar and wind energy by carefully accommodating their seasonal variations [2]. Wide spread custom of renewable energy sources in dispersed power generation and a great saturation level is expected in the near future. PV generators are exclusively becoming increasingly popular to supply remote loads [3] and grid connected schemes. There are two events for photovoltaic systems: 1) standalone systems and 2) grid-connected systems. Standalone systems are used in low-power application and use many battery banks for power registration [4]. Grid-connected applications are used for low and high power applications to feed the utility grid with renewable energy [5]. PV power is converted to AC and directly injected into utility grid. Grid-connected systems may be single-stage or two-stage systems as shown in Fig. 1. In two-stage systems, the first stage is a dc-dc boost converter for boosting the PV voltage and realizing MPPT, where the second stage is a DC-AC inverter that synchronizes the injected power with the utility grid power and transfers the collected power from the PV array to the AC grid [6]. However, two-stage systems have drawbacks, such as lower reliability, complication in control, larger size, higher cost, more power loss and lower efficiency. On the other hand, single-stage grid-connected systems offerd many advantages such as more efficiency, simple topology and economical than the two-stage system [7]. For PV systems, the PV power-voltage and voltage-current curves have a non-linear relationship. To maximize the output power from the PV system and to maximize its efficiency, it is indispensable to operate it at the maximum power point (MPP). MPPs are dependent on environmental variables such as sun insolation and module surface temperature. So that to achieve operation at MPP while conditioning the output power in harmony with the power grid is considered a large significant task in such systems. MPP position changes in with changes of weather conditions [8] . Many MPPT techniques have been developed such as perturb and observe method [9] and the incremental conductance method [10]. MPPT algorithm is done and controlled by many controllers as fuzzy logic controller [11] and neural network controller [12]. With a goal to match MPPT, this paper presents an implementation and expermental results to have it from PV as well as to increase the efficieny and performance of a single stage three-phase system connected to grid, where incremental conductance algorithm used in that this research. In the incremental conductance method, the controller must measure the incremental changes in array current and voltage to predict the effect of a voltage change. This method requires more computation in the controller, but it can track changing conditions more rapidly than the perturb and observe method (P&O) [13]. Like the P&O algorithm, it can produce oscillations in the power output. This method utilizes the incremental conductance (dI/ dV) of the photovoltaic array to compute the sign of the change in power with respect to voltage (dP/dV). The inverter model and control algorithm of MPPT are developed and simulated in the Matlab/Simulink SimPowerSystem blockset environment and then linked to the prototype inverter by utilyzing the dSPACE MicroLabBox controller board. This paper is organized as follows: section 2 describes the system description; section 3 presents the mathematical model of PV; section 4 describes the control system of three-phase Grid-Connected PV System; section 5 shows the simulation followed by the corresponding discussion; section 6 shows the expermintal results; and finally, the conclusions are given in section 7 .

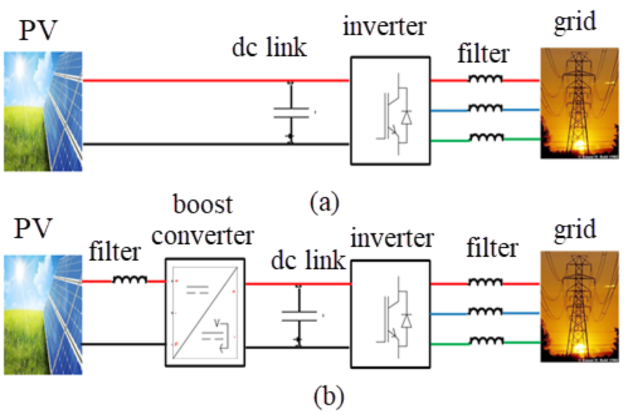

Fig .1. PV grid tied classification according to number of stages
(a) single stage system (b) two stages system

II. SYSTEM DESCRIPTION

Single-stage structure is used to remove the DC/DC converter, increase the efficiency, and reduce the overall system cost. Fig. 2 shows the block diagram of the suggested system. The system contains PV arrays, DC link capacitor, a three- phase voltage source inverter, three- phase inductance, three-phase step up transformer and utilty grid. Three control loops are implemented concerning MPPT controller, voltage control loop and current control loop.

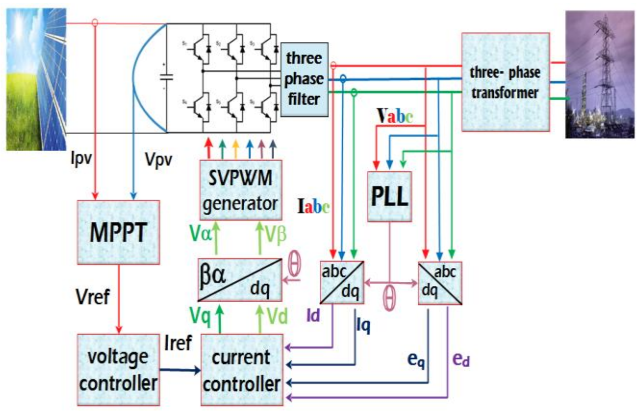

Fig .2. Block graph of single stage three -phase inverter

1. Photovoltaic generator Model

Fig. 3 shows equivalent circuit of one photovoltaic array [14]. Features of PV system is described as follows:

$$I_{PV} = I_d + I_{RP} + 1 \quad (1)$$

$$I = I_{PV} - I_O \left[\exp\left(\frac{V + R_s I}{V_{th} n} \right) - 1 \right] - \frac{V + R_s I}{R_p} \quad (2)$$

$$V_{th} = \frac{N_s KT}{q} \quad (3)$$

$$I_O = I_{o,n} \left(\frac{T_n}{T} \right)^3 \exp\left[\frac{q * E_g}{n * K} \left(\frac{1}{T_n} - \frac{1}{T} \right) \right] \quad (4)$$

Where,
I: the output current.
V: the output voltage.
I_{pv}:is the generated current under a given insolation.
I_d: diode current.
I_{RP}: the shunt leakage current.
I0: the diode reverse saturation current.
N: the ideality factor (1.36) for a p-n junction.
R_s: the series loss resistance (.1 Ω).
R_P: the shunt loss resistance (161.34 Ω).
V_{th}: the thermal voltage.
Q: the electron charge (1.60217646×10^{-19}C).
K:the Boltzmann constant (1.3806503×10^{-23}J/K).
T: (in Kelvin) is the temperature of the p-n junction.
E_g: the band gap energy of the semiconductor (Eg ≈

1.1eV for the polycrystalline Si at 25ºC) .
$I_{0,n}$: the nominal saturation current.
T: the cell temperature.
T_n: is cell temperature at reference conditions.

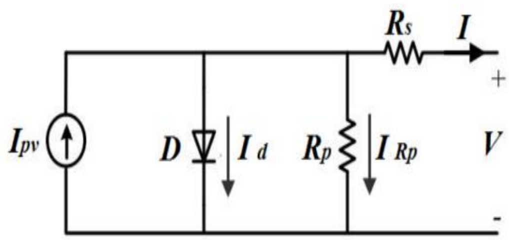

Fig. 3. Equivalent circuit of photovoltaic array

The following electrical characteristics of PV modules that were used are shown in Table 1, the array specifications at 1000w/m²-25ºc are shown in Table 2. The attendant power - voltage (P-V) characteristics under changing climatic conditions (temperature and radiation) are shown in Figs. 4a and 4b

Table 1. Electrical Specifications for the Solar Module Trina Solar TSM (295)

Parameter	Sympol	Value
Maximum Power	Pm	295W
Short circuit current	Isc	8.6A
Open circuit voltage	Voc	45V
Maximum power voltage	Vmp	36.5V
Maximum power current	Imp	8.08A
Number of parallel cell	Np	1
Number of series cells	Ns	72

Table 2 Array Specifications

Parameter	Symbol	Value
Total peak power	Ptm	2655W
Number of PV panels	N	9
Voltage input	Vm	360V

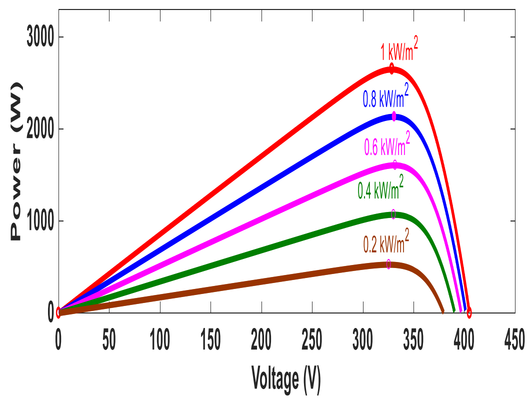

Fig. 4.a P-V characteristics of PV generator at varying radiation

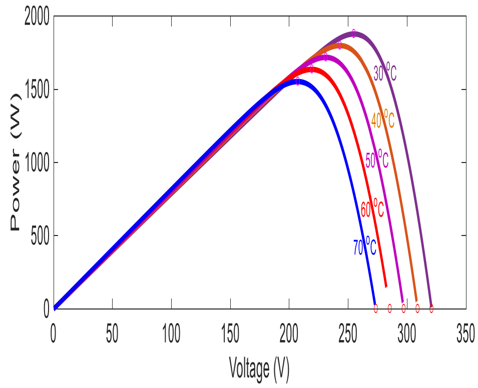

Fig. 4b P-V characteristics of PV generator at varying temperature

2. Mathematical Model of Three-phase Grid-Connected Inverter

The circuit topology of the grid-connected voltage source inverter (VSI) is shown in Fig. 5.

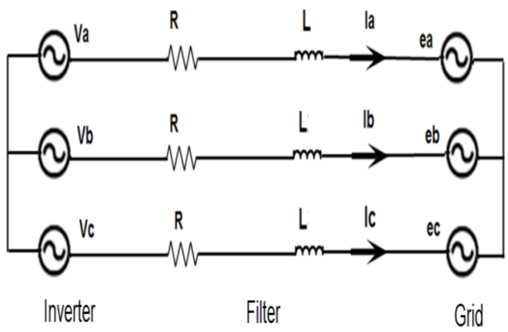

Fig. 5. Model of three- phase grid connected inverter

The assumption of symmetrical and balanced state of the grid voltage and zero grid impedance are presented; therefore, it can be expressed as,

$$\begin{bmatrix} ea \\ eb \\ ec \end{bmatrix} = \begin{bmatrix} V_m \sin \omega t \\ V_m \sin(\omega t - \frac{2\pi}{3}) \\ V_m \sin(\omega t + \frac{2\pi}{3}) \end{bmatrix} \quad (5)$$

The relation between VSI output voltages and line currents in the stationary reference frame is as follows:

$$\begin{bmatrix} ea \\ eb \\ ec \end{bmatrix} = \begin{bmatrix} V_a \\ V_b \\ Vc \end{bmatrix} - R \begin{bmatrix} I_a \\ I_b \\ Ic \end{bmatrix} - L \frac{d}{dt} \begin{bmatrix} I_a \\ I_b \\ Ic \end{bmatrix} \quad (6)$$

The stationary reference frame can be transformed into the dq rotating reference frame using parks transformation as: [14]

$$\begin{bmatrix} ed \\ eq \end{bmatrix} = \begin{bmatrix} Vd \\ Vq \end{bmatrix} - L \frac{d}{dt} \begin{bmatrix} Id \\ Iq \end{bmatrix} + \omega L \begin{bmatrix} -Id \\ Iq \end{bmatrix} - R \begin{bmatrix} Id \\ Iq \end{bmatrix} \quad (7)$$

Equation (7) can be communicated in the state space form as: [16]

$$\frac{dx}{dt} = A.X + B.U \quad (8)$$

Where the state vector [X], the input vector [U], the state matrix [A], and the input matrix [B] are defined as follows:

$$x = \begin{bmatrix} Id \\ Iq \end{bmatrix}, \quad U = \begin{bmatrix} V_d & V_q & e_d & e_q \end{bmatrix}^T \quad (9)$$

$$A = \begin{bmatrix} -\frac{R}{L} & \omega \\ -\omega & -\frac{R}{L} \end{bmatrix}, \quad B = \begin{bmatrix} -\frac{1}{L} & 0 & 0 \\ 0 & -\frac{1}{L} & \frac{1}{L} \end{bmatrix} \quad (10)$$

The advantages of operation in d-q synchronous reference frame is to deliver a method to control the active and reactive power independently. The active and reactive power are given by:

$$P_d = \frac{3}{2}(V_d I_d + V_q I_q) \quad (11)$$

$$P_q = \frac{3}{2}(V_q I_d - V_d I_q) \quad (12)$$

3. MPPT Control Algorithms

Incremental-conductance (INC) method

is found on the circumstance that the slope of the PV array power curve against voltage is zero at the MPP. The MPPT algorithm, which uses the INC method usually and has a fixed iteration step size determined by the INC, tries to develop the tracking time and to produce more energy on a vast irradiation changes environment. The MPP can be calculated by using the relative between dI/dV and –I/V. If dP/dV that is negative, then the MPPT is located on the right side of the current position and if it is positive, the MPPT is on left side [17]. The equation of INC method is:

$$\frac{dp}{dv} = \frac{d(\mathrm{v.I})}{dV} = I \frac{dV}{dV} + V \frac{dI}{dV} \quad (13)$$

$$\frac{dp}{dv} = I + V \frac{dI}{dV} \quad (14)$$

MPP is reached when dP/dV=0and

$$\frac{dI}{dV} = -\frac{I}{V} \quad (15)$$

$$\frac{dP}{dV} > 0 then V_P < V_{mpp} \quad (16)$$

$$\frac{dP}{dV} = 0 then V_P = V_{mpp} \quad (17)$$

$$\frac{dP}{dV} < 0 then V_P > V_{mpp} \quad (18)$$

If the maximum power point (MPP) during operation lies on the right side, dI/dV< -I/V and then the PV voltage must be decreased to reach the MPP [17]. INC method can be used to determine the MPP, improve the PV efficiency, and decrease power loss and system cost. INC algorithm can be seen in Fig. 6.

The oscillation around MPP area can also be suppressed in trade of with its implementation complexity.

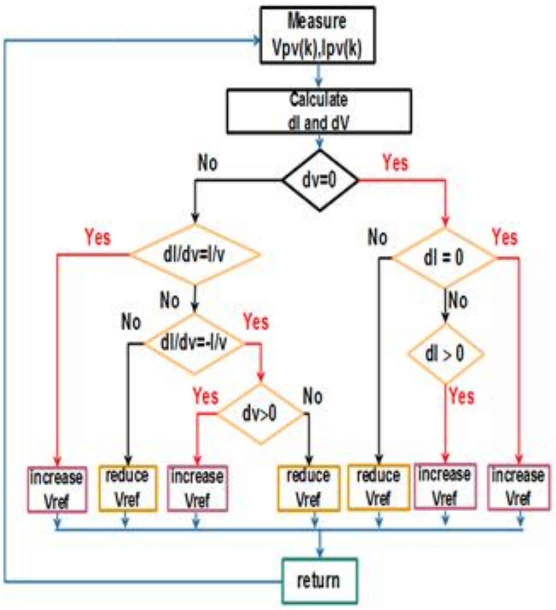

Fig.6. Flow chart of MPPT algorithm

4. Control of DC Link Voltage

DC link voltage is controlled via the voltage controller block as shown in Fig. 2. The controller regulates the dc-link capacitor voltage according to the reference voltage (vdc_{ref} =VPV_{ref}), decided by the MPPT scheme. The dc-link voltage regulation is achieved through the control of direct axis current, which in consequence, controls the real power injection into the grid. The main advantage of the single-stage construction is the operation at a variable dc-link voltage. The dc-link voltage has to track the PV array's MPP, which is controlled by the MPPT algorithm out of changing the dc-link reference voltage [18]. The estimated dc-link voltage reference (Vref) is processed through a voltage limiter and feeds a PI controller to establish a current command (current controller). Alternatively, the dc link voltage controller may be achieved by regulating the energy flow in and out of the dc-link capacitor.

5. Current Controller

MPPT algorithm for single-stage system is based on dc-link control capability of the inverter. Voltage control loop outs d-axis reference current (Id-ref) that is used as reference current to the current controller. By controlling the Id, the active power injected to the grid can be controlled, whereas the q-axis reference is set to zero for unity power factor operation [19]. In this paper, PI current controller is used due to its inherent simplicity as it gives good results.

III. SIMULATION AND EXPERIMENTAL RESULTS

1. Simulation Results

To investigate the performance of the proposed schemes using the INC method, a simulation model is developed for the overall system in Matlab/Simulink. The parameters of the simulated model are as follows: the output filter inductance is 5mH per phase, the line resistance is 0.01Ω, switching frequency is 10 kHz, nominal grid frequency is 50 Hz, dc-link capacitance value is 3300 µF, and the three phase peak line voltage of the grid is 156 V. Fig. 7 shows the theoretical results of the MPPT algorithm, where the PV voltage, current and input power are illustrated in the figure. In this figure, the starting point is at the open circuit of the PV string, where the voltage is maximum, the current is zero and the power is zero. Application of the algorithm pushs the system towards maximum power where the voltage is reduced to Vmp, the current is increased, and the power reaches its maximum value corresponding to the environmintal condition. That value of maximum power is 1000 watt depending on irradiance ($600w/m^2$) and temperature (35^0c). Fig. 8 shows the corresponding 3-phase injected current to the grid. The current waveforms are pure sinewave and free of fluctuations which means stability of the proposed controller.

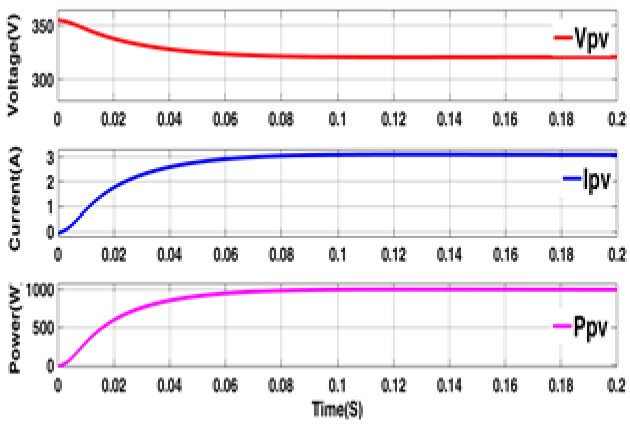

Fig.7 .Vpv, Ipv, Ppv waveforms during tracking.

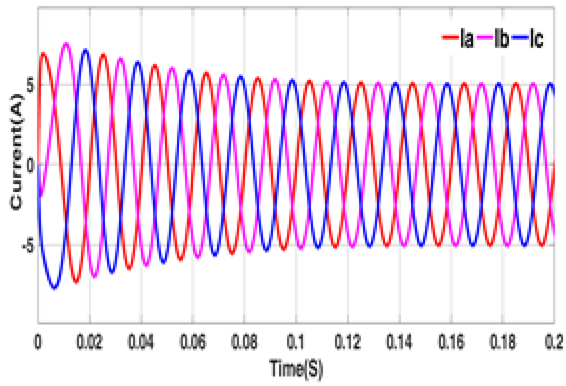

Fig. 8. 3-phase AC current injected to the grid.

2. Experimental Laboratory

The developed MPPT controller is designed and implemented using dSPACE MicroLabBox controller. Fig. 9 shows the experimental setup circuit that consists of PV array, step up transformer, three-phase inverter, dspace MicroLabBox, card of voltage and current sensor and filter by using solar irradiance and solar temperature instruments whose values are (600w/m² and 35⁰c).

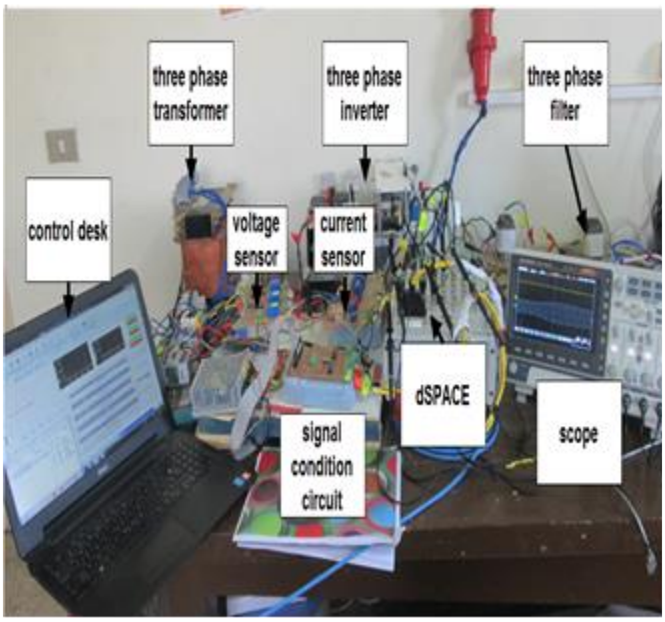

Fig.9. Expermental setup circuit

3. Experimental Results

Fig. 10 shows the experimental results of MPPT algorithms applied to the proposed system. The figure shows the PV voltage, current and PV output power, where the voltage of the PV decreases from open circuit (360V) and reaches the MPP value (320V), the output current increases from (0A) to (2.2A), and the output power increases to (1000 watt) maximum power point. The system moving towards the maximum power steady without oscillation or fluctuation and it matches the MPP at 3 seconds. Fig. 11 illustrates the expermental results of three phase current injected to grid by MPPT algorithm. The simulation and experimental results indicated that the system can achieve MPPT by sensing voltage and current of PV that is the input of MPPT algorthim. This figure also proves the stability of the output current and power from the system and illustrates the stability of the controller applied to the proposed system.

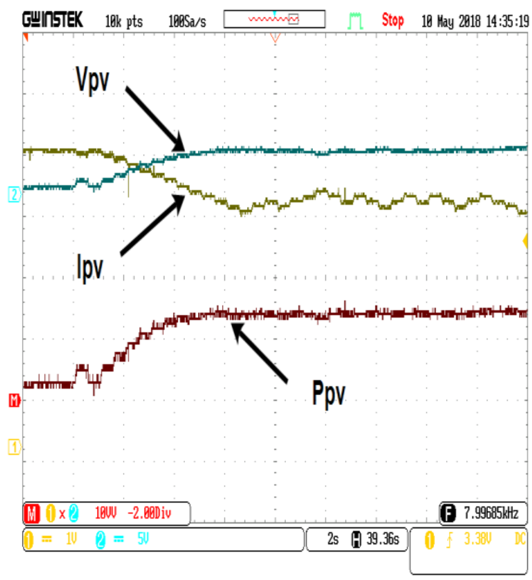

Fig. 10 .PV voltage, current, and input power [70V/div, 5A/div, 700W/div, 2s/div].

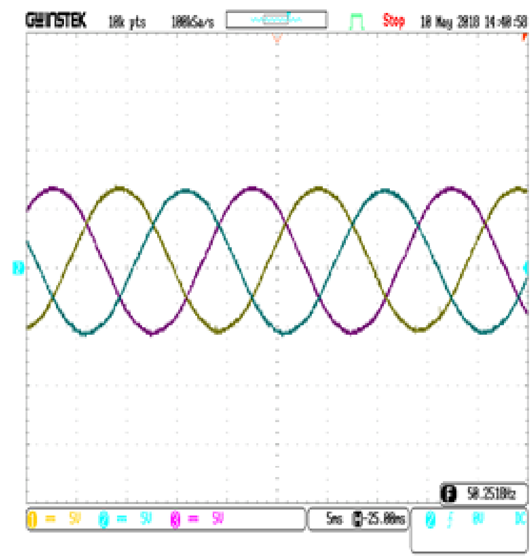

Fig. 11. three phase current injected to the grid [5A/div, 5ms/div].

IV. CONCULSION

Implementation of single stage three phase grid connected PV system is presented in this paper. In order to check the theoretical results, an experimental prototype was built. The developed MPPT algorithm was validated through the experimental results, Based on the simulated and the experimental results, the developed algorithm can track the PV MPP with a high degree of accuracy and stability, it can reach the MPPT at 3 seconds. Due to the simplicity and the low cost productivity of the developed algorithm, it is attractive for single-stage three phase grid connected PV systems.

REFERENCES

[1] M. Bilgili, A. Ozbek, B. Sahin and A. Kahraman. “An overview of renewable electric power capacity and progress in new technologies in the world.” Renewable and Sustainable Energy Reviews, vol. 49, 2015, pp 323-334..

[2] A. Buonomano, F. Calise, M. D. d'Accadia and M. Vicidomini. “A hybrid renewable system based on wind and solar energy coupled with an electrical storage: Dynamic simulation and economic assessment.” Energy, vol. 155, pp.174-189, 2018, doi.org/10.1016/j.energy.2018.05.006.

[3] A. Ba, E. Aroudam, O. E. Chighali, O. Hamdoun and M.L. Mohameda. “Performance optimization of the PV pumping system. ” Procedia Manufacturing, vol. 22, pp. 788-795, 2018, doi.org/10.1016/j.promfg.2018.03.112.

[4] L.W. Chong, Y.W. Wong, R.K. Rajkumar and D. Isa. “Modelling and simulation of standalone PV systems with battery-supercapacitor hybrid energy storage system for a rural household.” Energy Procedia, vol. 107, pp. 232-236, 2017, doi.org/10.1016/j.egypro.2016.12.135.

[5] R. Hasan, S. Mekhilef, M. Seyedmahmoudian and B. Horan. “Grid-connected isolated PV microinverters: A review.” Renewable and Sustainable Energy Reviews, vol. 67, pp. 1065-1080, 2017, doi.org/10.1016/j.rser.2016.09.082.

[6] P. Li, W. Gu, L. Wang, B. Xu and W. Shen. “Dynamic equivalent modeling of two-staged photovoltaic power station clusters based on dynamic affinity propagation clustering algorithm.” International Journal of Electrical Power & Energy Systems, vol. 95, pp. 463-475, 2018, doi.org/10.1016/j.ijepes.2017.08.038.

[7] O.M. Arafa, A.A. Mansour, K.S. Sakkoury, Y.A. Atia and M.M. Salem. “Realization of single-phase single-stage grid-connected PV system. ” Journal of Electrical Systems and Information Technology, vol. 4, Issue 1, pp.1-9, 2017, doi.org/10.1016/j.jesit.2016.08.004.

[8] M. A.M. Ramlia, E. Prasetyono, R.W. Wicaksana, N.A. Windarko, K. Sedraoui and Y.A. Al-Turki. “On the investigation of photovoltaic output power reduction due to dust accumulation and weather conditions. ” Renewable Energy, vol. 99, pp. 836-844, 2016, doi.org/10.1016/j.renene.2016.07.063.

[9] J. Ahmed and Z. Salam. “An improved perturb and observe (P&O) maximum power point tracking (MPPT) algorithm for higher efficiency.” Applied Energy, vol. 150, pp. 97-108, 2015, doi.org/10.1016/j.apenergy.2015.04.006.

[10] A. Loukriz, M. Haddadi, S. Messalti. “Simulation and experimental design of a new advanced variable step size incremental conductance MPPT algorithm for PV systems.” ISA Transactions, vol. 62, pp. 30-38, 2016, doi.org/10.1016/j.isatra.2015.08.006.

[11] Y-T. Chen, Y.-C. Jhang and R-H. Liang. “ A fuzzy-logic based auto-scaling variable step-size MPPT method for PV systems .” Solar Energy, vol. 126, pp. 53-63, 2016, doi.org/10.1016/j.solener.2016.01.007.

[12] H. Boumaaraf, A. Talha and O. Bouhali “A three-phase NPC grid-connected inverter for photovoltaic applications using neural network MPPT.” Renewable and Sustainable Energy Reviews, vol. 49, pp. 1171-1179, 2015, doi.org/10.1016/j.rser.2015.04.066.

[13] E.S Sreeraj, K. Chatterjee, and S. Bandyopadhyay. “One-cycle-controlled single-stage single-phase voltage-sensorless grid-connected PV system” IEEE Transactions On Industrial Electronics, vol. 60, no. 3, pp.1216-1224 March 2013.

[14] J.A. Ramos-Hernanz, J.J. Campayo, J. Larranaga, E. Zulueta, O. Barambones, J. Motrico, U.F. Gamiz, I. Zamora."Two photovoltaic cell simulation models in Matlab/Simulink." International Journal on Technical and Physical Problems of Engineering (IJTPE), vol. 4, no. 1, Issue. 10, pp.45-51, 2012.

[15] S.A. Lakshmanan, A. Jain and B.S. Rajpourhit. "A novel current controlled technique with feed forward DC voltage regulator for grid connected solar PV system," Power Systems Conference (NPSC), 2014 Eighteenth National.

[16] L.P. Sampaio, M.A.G. de Brito, G. de A. e Melo and C.A. Canesin. "Grid-tie three-phase inverter with active power injection and reactive power compensation." Renewable Energy, vol. 85, pp. 854-864, 2016.

[17] R.I. Putri, S. Wibowo and M. Rifa'i, "Maximum power point tracking for photovoltaic using incremental conductance method," Energy Procedia, vol. 68, pp. 22-30, 2015.

[18] W.J. Praiselin and J.B. Edward."Voltage profile improvement of solar PV grid – connected inverter with micro grid operation using PI controller," Energy Procedia, vol. 117, pp. 104-111, 2017, doi.org/10.1016/j.egypro.2017.05.112.

[19] P.M. Almeida, P.G. Barbosa, J.G. Oliveira, J.L. Duarte and P.F. Ribeiro. "Digital proportional multi-resonant current controller for improving grid-connected photovoltaic systems." Renewable Energy, vol. 76, pp. 662-669, 2015, doi.org/10.1016/j.renene.2014.11.087.

Journal of Renewable Energy and Sustainable Development (RESD) Volume 4, Issue 2, December 2018 - ISSN 2356-8569
http://dx.doi.org/10.21622/RESD.2018.04.2.065

DETECTABLE SYSTEM OF RESISTANCE OF VERTIMEC (ABAMECTIN) WITHIN THE TWO-SPOTTED SPIDER MITE, *TETRANYCHUS URTICAE* KOCH

Rania Ahmed Abd El-Wahab
Plant Protection Research Institute, Agricultural Research Center, EGYPT
rania-proline@hotmail.com

***Abstract* -** Augmented resistance of pesticides remains a principal issue for unsatisfactory impacts on the environment. So, there is a need to distinguish it faster by innovated devices and then find effective tools to reduce it as soon as possible, especially for mites such as *Tetranychus urticae*. Detectable tools, which are powered with solar energy, were used to discover Vertimec resistance depending on the assurance of the changes of electromagnetic field forces in comparison with sensitive mites. Acquired results with certain differences of electromagnetic forces were affirmed by evaluation of resistance proportions (RRs) which recorded 8.52- and 4.53-folds for resistant strains of Vertimec (Abamectin) on cotton and soybean, respectively, upon Vertimec LC50s. Furthermore, they were 5.97- and 4.29- folds for field Vertimec strains on cotton and soybean, respectively. However, there were no significant differences between resistan and field strains; they appeared in comparing the mentioned strains with susceptible mites. It may be well concluded that pesticides' resistance is now available to be detected by utilizing a simple and quick framework in the field.

***Keywords* -** Detector, Electromagnetic, *Tetranychus urticae*, Resistance and Vertimec.

I. INTRODUCTION

Resistance of pesticides is an essential subject particularly when it is related to the two spotted spider mite, *Tetranychus urticae*. It is vital to take the most important components of climate changes as top priority when resistance is the issue which agriculturists should give a hand to. In Egypt, with elevated ratios of CO_2 and UV pro rata with pesticides' resistance specifically of spider mites, it is difficult to control them with pesticides (Nahar *et* al. 2005) due to their short life cycle, reproduction high capacity, and ability to create protection from miticides (Georghiou 1990).

Even with the broad utilization of chemical pesticides, pests existed a noteworthy explanation behind crop production calamity worldwide. Common used pesticides caused numerous ecological, agricultural, medical, and financial problems. Imperatively, development of resistance occurred as a result of the overwhelming utilization of synthetic insecticides and the selection pressure on insects and mites.

Particular metabolic pathways utilized by insects to change over hindrances into less poisonous structures or their expulsion from the framework are featured. Utilizing the proteomics approach, responsible proteins affected by pesticides in insects and then their alterations by pesticides' resistance could be distinguished (Dawkar et al., 2013).

The available tool to assay pesticides' resistance is depending on Immunochromatographic dip-stick-format kits. They were created to distinguish resistance to carbamates and organophosphates and others. Strips were upon polyclonal antisera versus resistance of pesticides which are related to esterase isozymes isolated from insects. They were simply used by farmers anywhere (Kranthi, 2005), but the problem which is related to cost and accuracy still exists.

Using electromagnetic fields as traps or even to attract or eject pests, is an ordinary known process. It was started by Gerharz (1991) who situated the electromagnetic field nearby or in a pest control. A gadget was chosen from the gathering comprising insect traps, insect teasing stations containing a pest poison, and pointer stations. For instance, a wide assortment of regular pest traps for slithering insects could be retrofitted with an electromagnetic field generator. Devices could have the generator to a focal area of a trap with an electromagnetic field generator, contained or not, a chemical or biological attractant.

http://dx.doi.org/10.21622/RESD.2018.04.2.065

So, there is a need to get a priceless device that would be able to get fast and accurate results to help farmers to discover the problem in the beginning before its development. In the same time, there will be a new use of electromagnetic fields to detect pesticides' resistance in order to protect the environment of more quantities of acaricides.

Mites with certain changes in their bodies provided electric changes and then with the present magnetism in the instrument, electromagnetics field are available to react effectively with exposed mites. Nevertheless, resulted electromagnetic fields' forces and their Axis Graph Magnetic Meter were assessed by the innovated instrument in order to detect pesticides' resistance easily and vastly as presented in this paper.

Image (1) Instrument Prototype Parts:

1-Solar Panel

2-Container of battery, microcontroller system (PIC16F627A), UGN3503U, EMI and others

3-Power

4- Blue Light Emitting Diodes (LEDs)

5- Red Light Emitting Diodes (LEDs)

II. MATERIALS AND METHODS

- **Innovated Instrument Components:**

The prototype of the instrument is shown in Image (1) with all of its components: A solar panel with its attachments and a DC-Motor. Electromagnetic field resulted from two magnets and with the passage of electric current, the required field was gained. Whenever the current is gone through mites, the electrophysiological differences appeared in changes of voltages at LCD monitor. Microcontroller system (PIC16F627A) was used to detect the resistance through electrochemical changes in the resistant strain in comparison with the other sensitive one. The sensor, UGN3503U was used to determine the magnetic field strength and varying voltage provided at output proportions which are picked up to the fielstrength. Also, Electromagnetic interference (EMI) detector was attached to the present circuit to provide and confirm accurate readings of the final electromagnetic field strength. Comparison appeared in the magnetic field force and the current conductance with attention to any differences in food resource, weather conditions, etc.

- **Maintenance of *Tetranychus urticae* strains:**

1. Susceptible strain

Colonies of the spider mite, *T.urticae* were raised under lab conditions (25 ± 2^0C, 60±5%RH and 12 hours light/12 hours dark) at Plant Protection Research Institute for several years without exposure to any contaminations or pesticides.

2. Resistant strain

Original colony of the spider mite, *T.urticae* was set up from mites gathered from castor oil plants without exposing to pesticides. It was raised under laboratory conditions (25 ± 2^0C, 60±5%RH and 12 hours light/12 hours dark) to assess the action of Vertimec (Abamectin $18\ g\ L^{-1}$ EC) against *T.urticae* grown-up females. The leaf-dip technique presented by Dittrich (1962) was utilized. All treatments were done under laboratory conditions and each was replicated thrice . Likewise, control discs were dipped in water only. Mortality percentages were determined and corrected by using Abbott's formula (1925). Pooled data were subjected to probit analysis (POLO PC) (LeOra software, 1994). The original strain females were selected for Vertimec for 20 generations according to Yang et al. (2002) with some modifications. 1000 adult females of this colony started this selection. Every two generations, LC50s and LC90s were evaluated. New LC50 was applied as subsequent selection pressure. The next selection transferred to untreated leaves. LC50 estimations of the selected strain were compared to those of the susceptible strain. LC50 of Field colony was got after exposure to the recommended concentrations of Vertimec under certain values of UV and CO2 which interacted with sprayed pesticide on infested cotton and soybean with *T.urticae*. Then, the resistance ratio (RR) was computed. Field colony was got after exposure to the recommended concentrations of Vertimec under certain values of UV and CO2 which interacted with sprayed pesticide on infested cotton and soybean with *T.urticae*.

- **Determination of electromagnetic fields:**

Samples of *T.urticae*, about 100 adult females, were placed inside the instrument. Resistan and field strains were compared with the control which was reared on cotton and soybean leaves. Differences of electromagnetic fields' forces and Axis Graphs appeared and were recorded by the microcontroller system.

- **Data Analysis**

SPSS (V.16) was used to show differences among resistant, field and susceptible strains under electromagnetic' forces instrument. Jonckheere-Terpstra Test, Friedman Test, Kendall's W and others were used to test significance between resistance and susceptible cases at probability with 5% and 1%.

III. RESULTS AND DISCUSSION

Data revealed that strength of electromagnetic fields was changed particularly with significant differences between resistant and susceptible mites as appeared in Figure (1). Direct determination recorded high strength of electromagnetic fields in case of resistant mites to Vertimec on cotton followed by resistant strain on soybean with 45.37 and 28.14 G, respectively.0020 Therefore, there were specific differences in Axis Graph Magnetic Meter resulted of electromagnetic fields through both resistant and susceptible of adult females of *T.urticae* on certain crops as appeared in Figure (2).

Jonckheere-Terpstra Test showed that Std. Deviation of J-T Statistic=.957* among grouping variables of mites. Therefore, both Chi-Square and Median were =3.000a and 28.140 [a]. While, Kruskal-Wallis Test showed that Chi-Square=2.000 [b] at 5%. Proximity Matrix proved that a dissimilarity matrix with 51.587 as euclidean distance among variables while a similarity matrix was determined by the correlation between vectors of values was -.997.

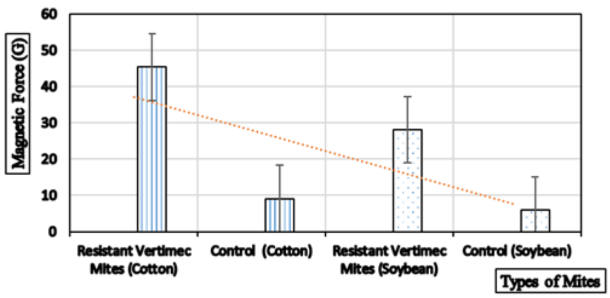

Fig .1. Force of resulted electromagnetic fields through both resistant and susceptible of adult females of *T.urticae* on certain crops

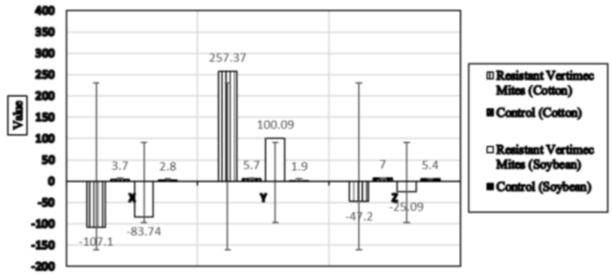

Fig .2. Axis Graph Magnetic Meter resulted of electromagnetic fields through both resistant and susceptible of adult females of *T.urticae* on certain crops

Subsequently, toxicity of Vertimec was compared both of field and resistant strains with the susceptible strain of *T.urticae* on cotton. Whereas, LC_{50} values were 1542.91, 1915.47and 258.45μLL^{-1}, respectively, which showed that LC50 of cotton field strain exposed to moderately levels of CO_2 and UV recorded so close value to that of 20th generation of the laboratory resistant strain. The same situation was in the case of $LC_{90's}$ which recorded 14207.39, 16328.37and 1420.74μLL^{-1}, respectively. Relative to the laboratory strain (S), the resistant ratios (RR) to Vertimec for *T.urticae* laboratory resistant strain and field strain, shown at Table (1). RR's at Vertimec $LC_{50's}$ were 5.97- folds and 8.52- folds, respectively. The same trend occurred in case of assessment of Vertimec resistance in *T.urticae* strain on soybean.

Data showed that LC50 values were 4013.25, 4220.17 and 198.82 μLL^{-1}, respectively, which showed that LC50 of cotton field strain exposed to moderately levels of CO_2 and UV recorded a so close value to that of 20th generation of the laboratory resistant strain. The same situation was in the case of $LC_{90's}$ which recorded 17210.74, 19102.35 and 780.34 μLL^{-1}, respectively. Relative to the laboratory strain (S), the resistant ratios (RR) to Vertimec for *T.urticae* laboratory resistant strain and field strain are shown at Table (1).

RR's at Vertimec $LC_{50's}$ were 5.97- folds and 8.52-folds, respectively. The same trend occurred in case of assessment of Vertimec resistance in *T.urticae* strain on soybean. Data showed that LC_{50} values were 4013.25, 4220.17 and 198.82 μLL^{-1}, respectively, which showed that LC_{50} of cotton field strain exposed to moderately levels of CO2 and UV recorded a so close value to that of 20th generation of the laboratory resistant strain. The same situation was in the case of $LC_{90's}$ which recorded 17210.74, 19102.35 and 780.34 μLL^{-1}, respectively. Relative to the laboratory strain (S), the resistant ratios (RR) to Vertimec for *T.urticae* laboratory resistant strain and field strain are shown at Table (2). RR's at Vertimec $LC_{50's}$ were 4.29- folds and 4.53- folds, respectively. According to Hayashi scale (1983), RRs of both strains resistant to Vertimec LC_{50}, infested cotton and soybean, could be ranked as low resistance. Friedman Test proved the highest significant effect of certain crops on LC50s values at 1% (Chi-Square =12.684**). Kendall's Coefficient of Concordance (Kendall's W^a) = .705** with highly significant Chi-Square =12.684 at 1%.

Table 1. Assessment of Vertimec toxicity against certain strains of adult females of *T.urticae*

T.urticae Strains	Crops	Vertimec Lethal Concentrations				LC90/LC50 Ratio
		LC_{50}		LC_{90}		
		Main μLL^{-1}	*RR_{50}	Main μLL^{-1}	*RR_{90}	
Field	Cotton	1542.91^a	5.97	14207.39^a	9.99	9.21
Resistant		1915.47^a	8.52	16328.37^a	11.49	8.52
Susceptible		258.45^b		1420.74^b		5.50
Field	Soybean	4013.25^a	4.29	17210.74^a	22.10	4.29
Resistant		4220.17^a	4.53	19102.35^a	24.48	4.53
Susceptible		198.82^b		780.34^b		3.92

*Resistance ratio (RR) =LC50 or LC90 of Resistant Strain/ LC50 or LC90 of Susceptible Strain.

Pesticides resistance in *Tetranychus urticae* is a portent which caused by many reasons. One of their causes is the introduction of exceeding levels of UV and CO_2, which could assume a critical part to get a resistant field strain. Vertimec, an articulated miticide, LC50 of the research center safe strain which is kept up under selection pressure till F40 and the resistant field strain in comparison with susceptible strain were 2099.38, 200.01 and 50.822 μLL^{-1}, respectively. Additionally, the raised esterases and mixed function oxidases (MFO) in both the laboratory and the field resistant strains had basically characterized the impact of extensive radiation of UV on the surpassed resistance levels recorded for the two strains (Abd El-Wahab and Taha, 2014).

Consequently, expanded CO_2 and global warming can be relied upon to positively influence the concoction barrier flagging framework in plants. Those factors will render them more vulnerable pest assault. The expanded number of produced generations every year and incessant populace flare-ups of potential pests require ceaseless uses of high measure of pesticides. It will boost exposed mites and insects to create pesticides' resistance vastly (Petzoldt and Seaman, 2007). Further, prolongation of insects' lifespan is prolonged under high CO_2 and temperature. Besides, such climate variations will stabilize such insecticide resistant in assortments of pests in their populations. Therefore, all mentioned will make more prominent harm plants even under broad pesticides measures. Also, a few classes of pesticides have been appeared to be less powerful in controlling pests at higher temperatures (Musser and Shelton, 2005).

Vertimec (Abamectin) resistance in *T. urticae* was also reported by several authors (Beers et al., 1998). Stumpf and Nauen (2002) found that MFO (cytochrome P450-dependent monooxygenase) activity was higher in many strains of *T.urticae* than the susceptible strain. Consequently, Abamectin resistance was strongly synergized by PBO (piperonyl butoxide) and DEM (diethyl maleate), suggesting that MFO and GST (glutathione S-transferases) might be involved in abamectin resistance. Astonishingly, levels of cytochrome P450 monooxygenases, specifically, CYP6CM1 in mix with a simple to utilize counter acting agent identification framework permit a quick, dependable, and extremely touchy detection of pesticides' resistance to insects, and certainly to *Bemisia tabaci*, to Neonicotinoid and Pymetrozine (Nauen et al., 2013). Nevertheless, Li et al. (2016) demonstrated that RRs were ranged between 6.51 and 6.03 for *Myzus persicae* (Sulzer) infested tobacco, to certain pesticides in China. Results demonstrated that resistance ratios were RR = 6.51 and 6.03which meant populaces have created minor imperviousness to Imidacloprid. One populace (NC) has achieved a high resistance level to Cyhalothrin (RR = 41.28), five populaces indicated medium level (10.36 ≤ RR ≤ 20.45), and the other six stayed powerless (0.39 ≤ RR ≤ 3.53). As respects Carbosulfan, three populaces have created medium resistance, four populaces indicated just minor resistance, and the other five (0.81 ≤ RR ≤ 3.97) were as yet vulnerable. Populace SZ built up a medium level (RR = 14.83) to Phoxim, the other 11 were vulnerable (0.29 ≤ RR ≤ 2.41). To examine the potential resistance system, restraint impacts of synergists and detoxifying compound exercises were identified. The outcomes showed that the MFO was the most vital detoxifying catalyst presenting Imidacloprid resistance, and CarE was most imperative to Cyhalothrin, Carbosulfan and Phoxim. Our examination gave an exhaustive overview of insecticide resistance of *M. persicae* in Chongqing, and proposed that distinctive districts should take comparing administration to postpone the insecticide resistance advancement and draw out the convenience of insecticides.

Furthermore, magnetic fields were tested on mites, *Tetranychus urticae* and *Polyphagotarsonemuslatus latus* which infested tomato leaves and some leaves were passed through 500 Gauss magnetic field and others were sprayed with magnetic water (Al-Ani, 2010). Results showed the significant decrease of mites' individuals and raised numbers of mites' eggs. That was explained upon hyperactivation of some enzymes in exposed mites to lay down more eggs. Even though, magnetic water showed its effect on the preparation of spray liquids against on the viability of plant protection agents as shown by Wachowiak and Kierzek (2002). They reported raised effectiveness in the control of *Phytophthora sp*. infested potato, after the use of these fungicides diluted in magnetic water. Likewise, magnetic water incremented the efficacy of acaricides against *Tetranychus urticae*. They were Talstar, Omite, Magus and Omite by the use of one and three magnetizers, one magnetizer and two semi-rings (Górski et al., 2009).

In addition, development of exposure methods to certain magnetic field is developed at this paper. Electromagnetic field as shown could play an important role to detect resistance of pesticides in mites through an electromagnetic interference (EMI) detector by translating electrophysiological changes that occurred mainly at glutamate-gated chloride channels (GluCls) and γ-aminobutyric acid-gated rdl and glutamate-gated GluClα chloride channels (GABACl) and resulted to Vertimec' resistance in mites (Riga et al.,2017). Even though and according to other studies which suggested detoxification enzymes with no effective target site were able to cause abamectin resistance in field *T. urticae* populations (Çağatay et al.,2018).

Near future, all recorded readings would be collected and stored at the cloud to be available whenever needed through Internet of Things system (IOT). Besides, data base was connected and joined with resistance ratios (RRs) which were gained from both fields and laboratory' data. Such system will be easier to be used by farmers wherever they are being. But utilizing the electromagnetic fields depending on physiological differences in resistant mites is appeared to be newly emergence trial through this paper. Besides, the solution of metabolic resistance in mites is already done by exposure to specific colors of light emitting diodes (LEDs). Each color could be linked to reduce metabolic pesticides resistance in specific pest on certain plant (Abd El-Wahab,2015; Abd El-Wahab and Abouhatab,2014; Abd El-Wahab and Bursic,2014; Abd El-Wahab et al.2014). Hence, LEDs with different colors are able to be connected with the full innovated system to do the two required steps: firstly, to detect the pesticides' resistance and secondly to stop or reduce it effectively.

IV. CONCLUSION

To conclude, as the pesticides' resistance is a big problem that leads to disasters affecting the environment, there is a new innovated instrument to detect and then reduce it. The solution is depending on differences in electromagnetic forces in resistant strains of *T.urticae* in comparison with susceptible strain. Then, resistance ratios have confirmed the presence of formed resistance. As a consequence, such device is capable to detect resistance to pesticides and farmers can count on it efficiently.

REFERENCES

[1] R.A. Abd El-Wahab. "Direct effects of light emitting diodes (LEDs) on the two-spotted spider mite, *Tetranychus urticae*." Int. J. Sci. Res. Agricul. Sci., vol. 2, pp.79-85, 2015.

[2] R.A. Abd El-Wahab. and E.E. Abouhatab. "Effects of light emitting diodes (LEDs) on the insect predators behavior against the two forms of *Tetranychus urticae*." Int. J. Chem. Biol. Sci. (IJCBS), vol. 1, no. 4, pp. 36-45, 2014.

[3] R.A. Abd El-Wahab and V. Bursic. "Light emitting diodes (LEDs) reduce Vertimec, resistance in *Tetranychus urticae* (Koch)." Int. J. Chem. Biol. Sci. (IJCBS), vol. 1, no. 3, pp. 28-40, 2014.

[4] R.A. Abd El-Wahab and T.M. Taha. "The relation between Vertimec resistance in the two-spotted spider mite, *Tetarnychus urticae* and climate changes in Egypt." Int. J. Chem. Biol. Sci., vol. 1, no. 3pp. 1-10, 2014.

[5] R.A. Abd El-Wahab, S. Lazic and V. Bursic. "Compatibility among insect predators and light emitting diodes (LEDs) against the two forms of *Tetranychus urticae* in greenhouses." Int. J. Chem. Biol. Sci. (IJCBS), vol. 1, no. 5, pp. 20-27, 2014.

[6] W.S. Abbott. "A method of computing effectiveness of an insecticides." J. Econ. Entomol., vol 18, pp.265-267, 1925.

[7] N. Al-Ani, "Effect of magnetic field on mites." J Al-Nahrain Univ., vol.13, no.3), pp.104-109, 2010.

[8] E.H.Beers, H. Riedl and J.E.Dunley. "Resistance to abamectin and reversion to susceptibility to fenbutatin oxide in spider mite (Acari: Tetranychidae) populations in the Pacific Northwest." J. Econ. Entomol., vol. 91, pp. 352-360, 1998.

[9] N.S. Çağatay, P. Menault, M. Riga, J. Vontasd and A. Recep. "Identification and characterization of abamectin resistance," in *Tetranychus urticae*, Koch populations from greenhouses in Turkey, Crop Protection, vol. 112, pp.112–117, 2018.

[10] V.V. Dawkar, Y.R. Chikate, P.R. Lomate, B.B. Dholakia, V.S. Gupta and A.P. Giri. "Molecular insights into resistance mechanisms of Lepidoptera insect pests against toxins." J. Proteome Res., vol. 12, no. 11, pp. 4727-4737, 2013.

[11] V. Dittrich. "A comparative study of toxicological test methods on a population of the two-spotted spider mite, *T.urticae*." J. Econ. Entomol., vol 55, pp. 633-648, 1962.

[12] G.P. Georgiou "Overview of insecticide resistance," in Managing Resistance to Agrochemicals Eds. MB Green, HM LeBaron, WK Moberg. pp. 18-41, American Chemical Society, 1990.

[13] R. Gerharz. "Pest dislodgement by electromagnetic fields". http://www. freepatentsonl ine.com/H000998.pdf ,1991.

[14] R. Górski , M. Wachowiakm and M. Tomczak. "The effect of water magnetized with negative magnetic field on effectiveness of selected zoocides in the control of two-spotted spider mite (*Tetranychus urticae* Koch)." J. Plant Prot. Res., vol. 49, no. 1, pp. 87-91,2009.

[15] A. Hayashi. "History, present status and management of insecticide resistance" in Pest Resistance to Pesticides. Eds J Fukami, Y Uesugi, K Ishizuka. pp. 31-53. Tokyo, Japan, Soft Science (Wash. D.C.), 1983.

[16] K.R. Kranthi, Insecticide resistance -monitoring, mechanisms and management manual, Nagpur, India: CICR and ICAC, Washington. 2005, Pp.153.

[17] LeOra Software. POLO-PC. A User's Guide to Probit or Logit Analysis LeOra Software, pp. 28, Berkeley, CA., 1994.

[18] Y. Li, , Z. Xu, L. Shi, L. He and G. Shen. . "Insecticide resistance monitoring and metabolic mechanism study of the green peach aphid, *Myzus persicae* (Sulzer) (Hemiptera: Aphididae),in Chongqing, China." Pesticide Biochem.Physiol, vol.132, pp.21-28, 2016.

[19] F.P. Musser and A.M. Shelton. "The influence of post-exposure temperature on the toxicity of insecticides to *Ostrinia nubilalis* (Lepidoptera:Crambidae)." Pest Manag Sci. vol. 61, pp. 508-510, 2005.

[20] N.Nahar, W. Islam and M.M. Hague."Predation of three predators on two-spotted spider mite, *Tetranychus urticae* Koch (Acari: Tetranychidae)." J Life Earth Sci. vol. 1, pp. 1-4,2005.

[21] R. Nauen, K. Raming and K.Wölfel. Online: 2013. Available: http://www. google.com/patents/WO20131826 13A1?cl=en.

[22] C. Petzoldt and A. Seaman. "Climate Change Effects on Insects and Pathogens. Fact Sheet." Online: 2007. Available: http://www.climateandfarming.org/clrcc.php.

[23] M. Riga, S. Bajda, C. Themistokleous, S. PapaDaki, M. Palzewicz, W. Dermauw, J. Vontas and T. Van Leeuwen. "The relative contribution of target-site mutations in complex acaricide resistant phenotypes as assessed by marker assisted backcrossing in *Tetranychus urticae*." Scientific Reportss, vol. 7, pp. 9202-9214, 2017, DOI:10.1038/s41598-017-09054-y

[24] N.Stumpf and R. Nauen. "Biochemical markers linked to abamectin resistance in *Tetranychus urticae* (Acari-Tetranychidae)." Pestic. Biochem. Physiol., vol. 72, pp. 111-121, 2002.

[25] M.Wachowiak and R. Kierzek. "Wpływ dawki środka ochrony roślin, dodatku adiuwanta i wielkości kropel na efektywność zwalczania agrofagów." Prog. Plant Protection/Post. Ochr.Roślin, vol. 43, no. 2, pp. 994–997, 2003.

[26] X. Yang, L.L.K. Buschmann, Y. Zhu and D.C. Margolies"Susceptibility and detoxifying enzyme activity in two spider mite species (Acari : Tetranychidae) after selection with three secticides." J. Econ. Entomol., vol. 95, pp.399-406, 2002.

Journal of Renewable Energy and Sustainable Development (RESD) Volume 4, Issue 2, December 2018 - ISSN 2356-8569
http://dx.doi.org/10.21622/RESD.2018.04.2.072

Improved Theoretical Conversion Efficiency of a Dual Junction GaInP/Si Mechanically Stacked Photovoltaic Cell

Debashish Pal
M.Tech., Department of Electronics and Communication Engineering, Institute of Engineering and Management, Kolkata, India
pal.debashish@gmail.com

***Abstract* -** Dual junction tandem solar cells can utilize the solar spectrum photons with a broader range of energies as compared to the conventional single junction solar cells; thereby demonstrating higher conversion efficiency. This paper deals with the numerical modeling of a dual junction GaInP/Si based multijunction tandem photovoltaic cell. The semi empirical modeling approach was used for simulation which produced a theoretical one sun conversion efficiency of over 30% for the proposed four terminal configuration.

***Keywords* -** ARC, Open Circuit Voltage, PC1D, Short Circuit Current, Tandem cell, TCO

I. INTRODUCTION

Multijunction solar cells are more sensitive to solar spectrum than single junction solar cells [1-2]. Single junction silicon based solar cells have reached their peak conversion efficiency limits in the field of photovoltaics [3]. However, stacking a silicon solar cell with a higher bandgap material solar cell enables theoretical one sun conversion efficiencies exceeding the 30% limit. A larger bandgap material on the top absorbs photons with higher frequencies ensuring reduction in the efficiency losses associated with the thermalisation process. The materials most suited for the development of high efficiency multijunction solar cells are the III-V compound semiconductors, where the lattice matching condition can be managed. Additionally, silicon as a substrate has the advantages of being relatively cheap and abundant as well as having good radiation resistance [4-5].

Mostly tandem cells use series connection of subcells resulting in two terminal devices. Boundary condition associated with two terminal configuration requires that the current in both the subcells remains equal. For the power output to reach the maximum under these conditions exact current matching is required. This can be achieved by adjusting the thickness and doping concentration of different layers. The power deliverable to an external load is strongly limited by the efficiency of the top cell. In a four terminal configuration however, the operating points of the subcells can be controlled independently ensuring maximum transfer of power. In a four terminal configuration, the maximum power of each subcell is independent of one another, therefore, the electrical matching remains optimal. Four terminal mechanically stacked GaInP/Si cells are connected by an adhesive which allows higher degree of flexibility in terms of circuit wiring [6-8].

II. MODELING

In this paper, semi empirical modeling was used to demonstrate the performance of GaInP/Si dual junction solar cell. The GaInP and silicon sub-cells were simulated independently each at its own maximum power point. Unlike the monolithic multi-junction devices there is no need for the current matching between the sub-cells here as it is a four terminal configuration.

The integration of the GaInP cell with the Si cell reduces the intrinsic limitation associated with the standalone Si cell. Conversion of the short wavelength radiation associated with the solar spectrum can be achieved by the GaInP cell while the conversion of the longer wavelength radiation is taken care of by the Si cell.

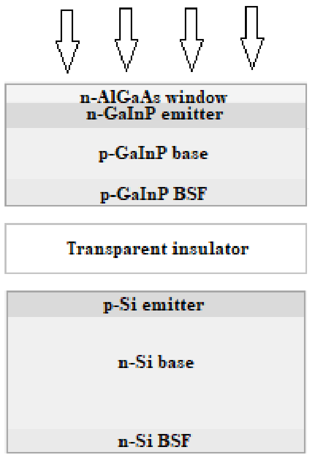

Fig .1. Schematic diagram of the four-terminal photovoltaic cell

Fig. 1 shows the schematic diagram of the dual junction tandem solar cell which comprises a GaInP based top cell of thickness 1.7 µm and a silicon-based bottom cell having thickness of 230 µm. The top cell has an AlGaAs based wide bandgap (2.1eV) window material having variable thickness. Each of the subcells has uniformly doped emitter and base layers of variable thickness and doping concentrations. To generate an electric field barrier for the minority carriers, the top and the bottom subcells have back surface field (BSF) layers of adjustable doping concentration and thickness. The electric field avoids the possibility of surface recombination. However, these adjustments are made keeping the total thickness of the top and the bottom cells constant at 1.7 µm and 230 µm, respectively [9]. In practice, to avoid the inherent optical losses associated with the mechanically stacked solar cells, electrically insulating and optically transparent adhesives are used to bond the cells.

For the sake of simplicity, the structure used for electrical characterization does not incorporate any defects at the interface and the surface or losses related to the tunnel junction (for the two terminal configuration) and the insulation. The operating temperature was chosen to be 25ºC with a device area of 1cm^2. The optimization of the sub-cells was performed under AM1.5G one sun illumination condition having an intensity of 0.1W/cm^2. The modeling and simulations were performed using PC1D simulation software [10], which is a computer program used for modeling crystalline semiconductor devices with emphasis on photovoltaic devices and is used as a simulation tool to understand the operation of solar cells yielding reliable results. The parameters used in the simulation are taken from reference [9]. The GaInP top cell has a ZnS anti-reflection coating on the front side and the Si bottom cell has a TCO coating on the front face (not shown in fig. 1). The ZnS and the TCO coatings on the front side of the cells have been optimised using simulations. The modelling considers a 1.7µm thick GaInP cell and a 230µm thick Si cell with constant light trapping.

III. RESULTS AND DISCUSSION

Historically, AlGaAs/Si dual junction solar cell has achieved 1-sun efficiency exceeding 21% by the epitaxial growth technique [11]. III-V/Si multi-junction solar cells were also demonstrated to achieve efficiencies of over 25% and 30% under 1-sun and 112-suns by means of direct wafer bonding [12-13]. Mechanically stacked GaInP/InGaAs/Si based solar cell has been reported to achieve efficiency of over 27% under 1-sun [14].

Unlike the AlInP window layer, S. Essig, M. A. Steiner, C. Allebé, J.F. Geisz, B. Paviet-Salomon, S. Ward, A. Descoeudres, V. LaSalvia, L. Barraud, N. Badel, A. Faes, J. Levrat, M. Despeisse, C. Ballif, P. Stradins, D.L. Young, “Realization of GaInP/Si dual-junction solar cells with 29.8% one-sun efficiency”, an AlGaAs window layer having a dielectric constant of 10.63 is chosen over the GaInP top cell having a lattice mismatch of only 0.03%. The window layer has a uniform n-type doping concentration of 1x10^{17}atoms/cm^3. The thickness of the window layer is varied to find the optimum value of efficiency.

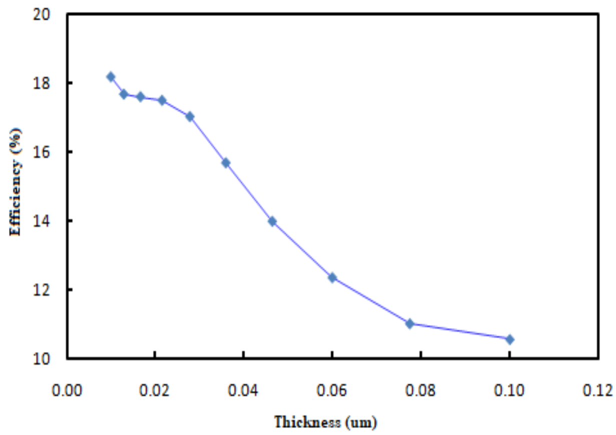

Fig .2. Window layer thickness vs. efficiency

The result of the simulation (Fig. 2) indicates that the efficiency is at a maximum value of 18.17% when the thickness of the window layer is at 0.01µm.

A study to determine the influence of the thickness of the ZnS anti-reflection coating on the fraction of photon current absorbed and reflected for the GaInP cell was performed. The incident light passes through the ZnS anti-reflective coating (refractive index=3.805-2.252) and the AlGaAs window layer (refractive index=1.368-3.124) before reaching the GaInP substrate. This structure causes a refractive index mismatch which makes the ZnS ARC layer less reflective. A similar examination was conducted for the bottom cell having a TCO layer (refractive index=2.447-1.953) on top of the Si substrate. For different values of the ZnS and TCO layer thickness, the fractions of photon current absorbed and reflected are summarised in Table I.

Table I. Influence of the ZnS and ITO Layers on the Percentage of Photons Absorbed and Reflected by the GaInP Cell and the Si Cell, Respectively

Cell	Thickness (µm)		Fractional Photon Current Absorbed (%)	Fractional Photon Current Reflected (%)	Efficiency (%)
GaInP	ZnS layer	10	68.7	28.6	13.7
		50	87.5	9.4	18.2
		100	70.8	25.8	14.3
		150	76.8	19.5	16.1
Si	ITO layer	10	72.9	0.5	13.3
		50	69.7	10.6	12.0
		100	62.3	15.9	11.1
		150	65.6	12.5	11.5

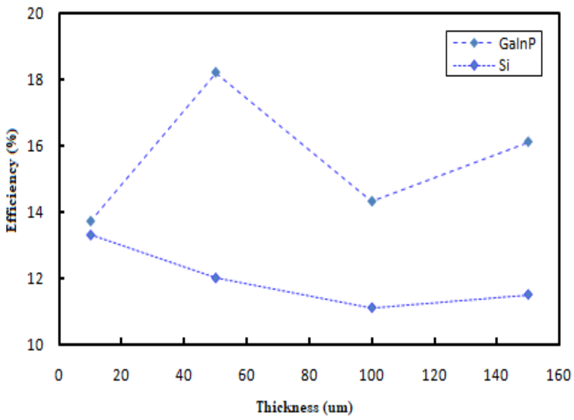

Fig .3. Dependence of efficiency on the thickness of ZnS ARC and ITO layer

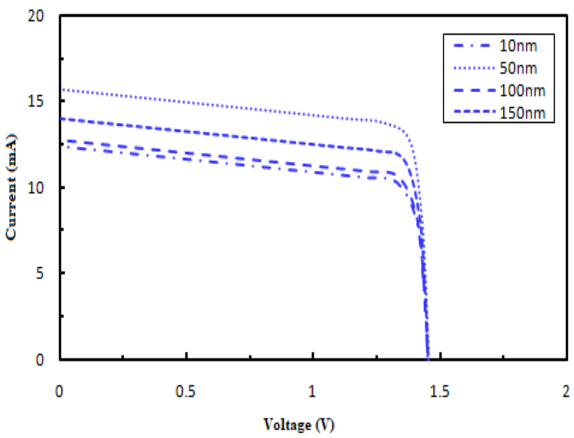

Fig .4. Current-Voltage characteristics of GaInP cell for different thickness of ZnS anti-reflective coating

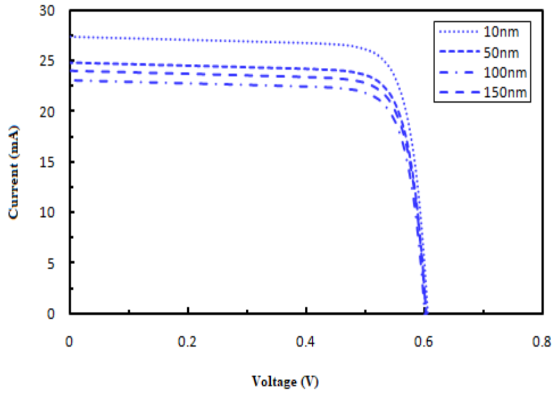

Fig .5. Current-Voltage characteristics of Si cell for different thickness of ITO layer

Fig. 3, 4 and 5 show that there is a strong dependence of the solar cell I-V characteristics on the thickness of the ZnS anti-reflection coating and the ITO layer. It can be observed from the I-V characteristics that for the GaInP cell the efficiency is maximum with a ZnS ARC coating thickness of 50nm. Also, the efficiency is maximum for an ITO layer thickness of 10nm for the Si cell. These results are in direct agreement with the data presented in Table I, which establishes that the percentage of photons absorbed by the base layer is greatest for the stated thicknesses.

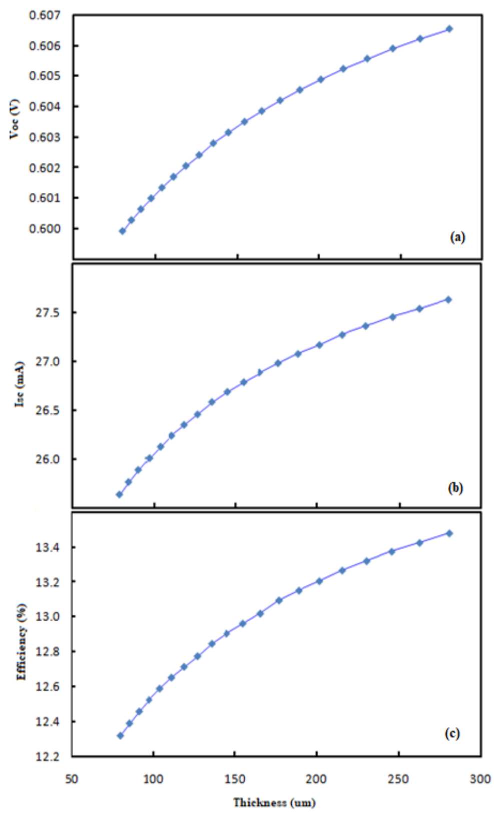

Fig .6. Influence of thickness of the Si bottom cell on (a) VOC (b) ISC (c) Efficiency

Journal of Renewable Energy and Sustainable Development (RESD) Volume 4, Issue 2, December 2018 - ISSN 2356-8569
http://dx.doi.org/10.21622/RESD.2018.04.2.072

Fig. 6 shows the dependence of the open circuit voltage, short circuit current and the efficiency on the thickness of the Si cell. As the thickness of the cell increases, the interaction of the incident photons with the cell improves. Thus, for greater cell thickness the incident photons generate a bigger number of electron-hole pairs, which in turn increases the overall photocurrent in the cell improving the efficiency.

Table II. Optimised Parameters of the Top and the Bottom Cell Used for the Final Design

Parameters	**Si Cell**	**GaInP Cell**
Thickness (µm)	230	1.7
Dielectric Constant	11.9	11.8
Bandgap (eV)	1.12	1.86
Emitter Thickness (µm)	10	0.1
Emitter Doping Concentration (/cm^3)	$1x10^{17}$ (p-type)	$5x10^{17}$ (n-type)
Base Thickness (µm)	215	1.49
Base Doping Concentration (/cm^3)	$1x10^{16}$ (n-type)	$1x10^{16}$ (p-type)
BSF Thickness (µm)	5	0.1
BSF Doping Concentration (/cm^3)	$1x10^{17}$ (n-type)	$4x10^{18}$ (p-type)
Front Surface Recombination Velocity (cm/s)	10000	10000
Rear Surface Recombination Velocity (cm/s)	10000	10000

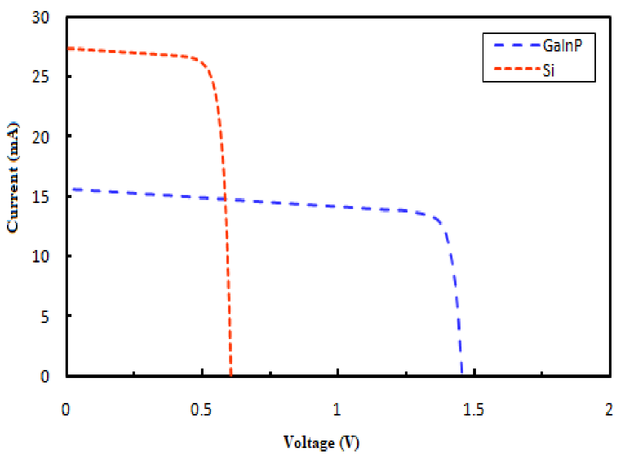

Fig .7. Current-Voltage characteristics of the optimised four-terminal photovoltaic cell

The theoretical model of the solar cell described in this investigation exceeds the experimental efficiency value of 25.6% [15] of a single junction Si solar cell. The efficiency of the tandem cell described in this paper is also close to the record one-sun efficiency of 31.1% [16] which was achieved with a monolithic GaInP/GaAs dual junction structure. The tandem cell theoretical efficiency of 31.5% for the structure under investigation in this paper is in close agreement with the practical efficiency of 29.8±0.6% obtained in S. Essig, M. A. Steiner, C. Allebé, J.F. Geisz, B. Paviet-Salomon, S. Ward, A. Descoeudres, V. LaSalvia, L. Barraud, N. Badel, A. Faes, J. Levrat, M. Despeisse, C. Ballif, P. Stradins, D.L. Young, "Realization of GaInP/Si dual-junction solar cells with 29.8% one-sun efficiency". An in-house efficiency of 31.5% was reported for a mechanically stacked interdigitated back contact dual junction solar cell. The Si bottom cell efficiency recorded therein was 12.5%, while the GaInP top cell demonstrated single junction efficiency of 19.1% [17]. Furthermore, it was shown that dual junction III-V/Si mechanically stacked and independently operated solar cell could reach cumulative one sun efficiencies of over 32% [18].

Table III: Summary of the Results

Cell	V_{OC} (V)	I_{SC} (mA)	Efficiency (%)
Si	0.6056	27.4	13.3
GaInP	1.455	15.7	18.2
Tandem	2.0606	15.7	31.5

IV. CONCLUSION

Studies performed on the mechanically stacked GaInP/Si based dual-junction solar cell structure achieved an accumulative one-sun efficiency of 31.5%. It can be observed that the overall efficiency of the solar cell is largely dependent on the efficiency of the top cell. The overall efficiency of the tandem cell is highly dependent on the thickness of the window layer, anti-reflection coating, ITO layer and the substrate thickness. Greater efficiencies can be achieved by increasing the open circuit voltage of the Si bottom cell and increasing the short circuit current of the GaInP top cell.

REFERENCES

[1] S.R. Kurtz, J.M. Olson and P. Faine. "The difference between standard and average efficiencies of multijunction compared with single-junction concentrator cells," Sol. Cells, vol. 30, no. 1–4, 1991, pp. 501–513,.

[2] P. Faine, S.R. Kurtz, C. Riordan and J.M. Olson. "The influence of spectral solar irradiance variations on the performance of selected single-

junction and multijunction solar cells," Sol. Cells, vol. 31, no. 3, 1991, pp. 259–278.

[3] D.D. Smith, P. Cousins, S. Westerberg, R. De Jesus-Tabajonda, G. Aniero and Y.-C. Shen. "Toward the Practical Limits of Silicon Solar Cells." IEEE Journal of Photovoltaics, vol. 4, no. 6, pp. 1465 –1469, 2014.

[4] M. Yang, T. Soga, T. Jimbo and M. Umeno. "High efficiency monolithic GaAs/Si tandem solar cells grown by MOCVD," in Proc of Twenty Fourth IEEE Photovoltaic Specialists Conference, vol. 2, 1994, pp. 1847-1850.

[5] J.F. Geisz, Olson, D.J. Friedman, K.M. Jones, R.C. Reedyand M.J. Romero. "Lattice-matched GaNPAs-on-Silicon tandem solar cells," in Proc of Thirty-first IEEE Photovoltaic Specialists Conference, 2005, pp. 695- 698.

[6] S. Essig, S. Ward, M.A. Steiner, D.J. Friedman, J.F. Geisz, P. Stradinsand D.L. Young. "Progress towards a 30% efficient GaInP/Si tandem solar cell," Energy Procedia vol. 77, 2015, pp. 464-469.

[7] J. Yang, Z. Peng, D. Cheong and R.N. Kleiman. "III-V on silicon multi-junction solar cell with 25% 1-Sun efficiency via direct metal interconnect and areal current matching," in Proc. of the 27th European Photovoltaic Solar Energy Conference and Exhibition, Frankfurt, Germany, 2012, pp. 160 -163.

[8] K.M. Gee and G.F. Virshup. "A 30%-efficient GaAs/silicon mechanically stacked, multijunction concentrator solar cell," Conference records of the 20th IEEE Photovoltaic Specialists Conference, Las Vegas, USA, 1988, pp. 754-758.

[9] S. Essig, M. A. Steiner, C. Allebé, J. F. Geisz, B. Paviet-Salomon,
S. Ward, A. Descoeudres, V. LaSalvia, L. Barraud, N. Badel, A. Faes,
J. Levrat, M. Despeisse, C. Ballif, P. Stradinsand D. L. Young, "Realization of GaInP/Si Dual-junction Solar Cells with 29.8% One-sun Efficiency." IEEE Journal of Photovoltaics, vol. 6, issue: 4, pp. 1-8, July 2016.

[10] PC1D, version 5.9, School of Photovoltaic and Renewable Energy Engineering at the University of New South Wales, Australia, 2008.

[11] T. Soga, K. Baskar, T. Kato, T. Jimboand M. Umeno. "MOCVD Growth of high Efficiency Current-matched A1GaAs/Si Tandem Solar Cell." Journal of Crystal Growth, vol. 174, pp. 579-584, 1997.

[12] S. Essig, J. Benick, M. Schachtner, A. Wekkeli, M. Hermle and F. Dimroth. "Wafer-bonded GaInP/GaAs//Si Solar Cells With 30% Efficiency Under Concentrated Sunlight." IEEE Journal of Photovoltaics, vol. 5, no. 3, pp. 977-981, 2015.

[13] K. Tanabe, K. Watanabe and Y. Arakawa. "III-V/Si hybrid photonic devices by direct fusion bonding," Scientific Reports, vol. 2, no. 349, pp. 1-6, 2012.

[14] J. Yang, Z. Peng, D. Cheong and R. Kleiman. "III-V on silicon multi-junction solar cell with 25% 1-sun efficiency via direct metal interconnect and areal current matching," Proc of the 27th European Photovoltaic Solar Energy Conference and Exhibition, Frankfurt, Germany, 2012, pp. 160-163.

[15] K. Masuko, M. Shigematsu, T. Hashiguchi, D. Fujishima, M. Kai, N. Yoshimura, T. Yamaguchi, Y. Ichihashi, T. Yamanishi, T. Takahama M. Taguchi, E. Maruyama and S. Okamoto. "Achievement of More than 25% Conversion Efficiency with Crystalline Silicon Heterojunction Solar Cell," IEEE Journal of Photovoltaics, vol. 4, pp. 1433-1435, 2014.

[16] M. Steiner et al., "article title," Proc of 41st IEEE PVSC (write full name), Tampa, USA, 2013, pp. 1429.

[17] M. Riennacker, M. Schnabel, E. Warren, A. Merkle, H.Schulte-Huxel, T.R. Klein, M.F.A.M. van Hest, M.A. Steiner, J. Geisz, S.K.-Schroder, R. Niepelt, J. Schmidt, R. Brendel, P. Stradins, A. Tamboli and R. Peibst. "Mechanically stacked dual-junction and triple-junction III-V/Si-IBC cells with efficiencies of 31.5% and 35.4%." in Proc of 33rd European PV Solar Energy Conference and Exhibition, 2017, pp1-4.

[18] S. Essig, C. Allebe, T. Remo, J.F. Geisz, M.A. Steiner, K. Horowitz, L. Barraud, J.S. Ward, M. Schnabel, A. Descoeudres, D.L. Young, M. Woodhouse, M. Despeisse, C. Ballif and A. Tamboli. "Raising the one-sun conversion efficiency of III-V/Si solar cells to 32.8% for two junctions and 35.9% for three junctions," Nature Energy, vol. 2, 2017, pp. 17-44.

Scan the QR Code

Journal of
Renewable Energy and Sustainable Development

RESD

Volume 4, Issue 2, December 2018 ISSN 2356-8569

ISSN 2356-8569

http://apc.aast.edu

مركز الأكاديمية للنشر
ACADEMY Publishing Center